Localization using a Particle Filter and Magnetic Induction Transmissions: Theory and Experiments in Air

Javier Garcia, Steban Soto, Arifa Sultana and Aaron T. Becker

***Abstract*— Localization is a key ability for robot navigation and collision avoidance. The advent of GPS has led to enormous improvements in terrestrial navigation. Unfortunately, EM waves propagate poorly through water, so navigation underwater remains challenging. This paper investigates estimating the relative location of a pair of triaxial coil antennas. By measuring the voltages induced in the receiving antenna when the transmitting antenna's coils are turned on sequentially, the distance between the antennas can be computed. Then, with knowledge of the current velocities of the antennas, we can apply a particle filter to generate an estimate of the location of the transmitting antenna with respect to the receiving one. The theory is supported by simulations and, as a first step, experiments performed in air are used to verify the theory.**

I. Introduction

Localization in underwater robotics is challenging due to the constraints imposed by the environment. Electromagnetic waves attenuate severely in sea water, rendering typical solutions for outdoor navigation impractical. Vision-based systems are susceptible to changes in water turbidity, while GPS systems require an above-ground base station and a wireless link to the robots for proper operation [1]. These wireless links typically rely on acoustic communications, which exhibit large range but suffer from low data rate, high propagation delay, multipath fading, and expensive transceiver costs.

A growing trend in physical-layer communications research is Magnetic Induction (MI) wireless communications. Loop antennas are used to transmit information through the near field [2]. As a result, the range for MI communications is low (under 10 meters underwater), but potential advantages include improved channel response, negligible propagation delay, and low-cost hardware implementation [3]. In particular, the low-cost of producing a MI transceiver is applicable to the design of underwater wireless sensor networks (USWN), where the installation and maintenance of loop antennas for communications reduces costs for large-scale deployment.

Autonomous maintenance or data collection in sensor networks present research problems that are related to coverage and path planning problems in robotics research. Specifically, we are interested in localization, the challenge of estimating the position and orientation of a robot in an environment based on sensor data. For this work, our sensors are triaxial antennas, which consist of three orthogonal coil loops in a sphere structure. Figure 1 shows a model of the triaxial antenna.

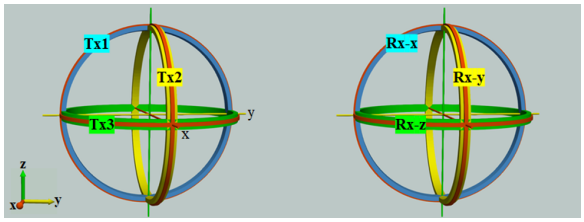

Fig. 1. The transmitter (TX) and receiver (RX) nodes are equipped with triaxial coil antennas, where three coils are orthogonal to each other. In our experiments, each coil is 0.20 m in diameter with 29 turns.

One major issue with localization with triaxial antennas is bearing uncertainty. This problem is caused from the fact that the only data that can be measured from the receiver coil is the induced voltage or current. For a stationary receiver with a single loop antenna, we are unable to tell if an approaching robot is coming from the left or right, since the received voltage is the same. As a result, two solutions for the location of the transmitter are possible. For triaxial coils, the number of potential solutions increases to as much as eight at certain configurations. This problem is often referred to as location ambiguity.

To mitigate this problem, we implement particle filters to estimate the location of the robot over time. Particle filters use sensor data to assign weights to a specified and constant number of estimates of a robot's location. If we assume the environment is known, these weights represent the probability that the estimate closely matches the actual location by comparing it to sensor readings. The estimates are resampled based on those weights. Over time, all estimates become closer to the robot's actual location.

This paper presents experimental results for the localization between two triaxial antennas. These experiments are done in air. We show the occurrence of location ambiguity and test the effectiveness of particle filters to estimate the position of the transmitter as it moves along a set of predetermined paths.

A brief survey of acoustic and magnetic induction localization techniques is presented in Section II. We describe the theoretical foundation of this work in Section III, then present our experimental setup in Section IV. The results for reconstructing the path of the transmitter using the particle filter in Section V. We conclude the work and discuss future plans in Section VI.

* This work was supported by the Texas Commission on Environmental Quality and the National Science Foundation under Grant No. [1646607].

Authors are with the Department of Electrical and Computer Engineering, University of Houston, Houston, TX 77204 USA {jgarciagonzalez, sssoto, asultan4, atbecker}@uh.edu

II. Related Work

The field of quasistatic magnetic positioning and tracking and positioning has a long history of developments. Pioneering work from [4] and [5] provide a framework for tracking and determining the position and orientation of triaxial source coils. De Angelis et. al have produced works in the combination of indoor and outdoor tracking systems [6] and the integration of GPS and magnetic positioning [7]. Other groups focus on the use of magnetic positioning for indoor tracking and navigation through walls [8], [9]. In recent work, Hehn et. al designed a system for localization and calibration for 5 degree-of-freedom systems [10], while Dumphart et. al studied the accuracy of quasistatic magnetic tracking systems [11].

This paper extends the work in [12], where the propagation of MI signals underwater was investigated, to address the challenge of localizing and tracking a triaxial coil antenna using range data only.

[4] provides a framework for tracking and determining both the position and orientation of a triaxial sensor coil relative to a triaxial source coil. The work demonstrates the applicability of the quasi-static approximation for low-frequency magnetic fields, representing the antenna as a magnetic dipole, and presents a method for linearizing the source-to-sensor coupling equations by using small-angle approximations. Because of the previous, large changes in the state of the antennas are difficult to track because the small-angle assumption does not hold.

Another approach for the localization of two triaxial antennas is explored in [13]. Here, the position vector of each antenna is computed from the 9 magnetic field components resulting from exciting the transmitting coils sequentially. Because the three elements of the vector are cosine terms there are a total of 8 possible solutions per coil, for a total of 16 points to be considered. The likelihood of the two position vectors is maximized through gradient descent. One important drawback is that the antennas must have different orientations to produce a good estimate.

For our approach, we take advantage of the quasi-static approximation for modeling our magnetic fields, and we also utilize the sequential method for obtaining 9 magnetic field readings using two triaxial antennas. However, our approach uses a faster method for computing the relative distance between the antennas, and then a particle filter produces an estimate based on the current velocities of the ROVs carrying them. This method is more robust against larger changes in state, and does not have constraints on the orientation of the antennas.

III. Theory

For this application we assume that the magnetic fields generated by the transmitting antenna are quasi-static due to the low frequency of the system (125[kHz]). This assumption allows us to model the coils as magnetic dipoles, which

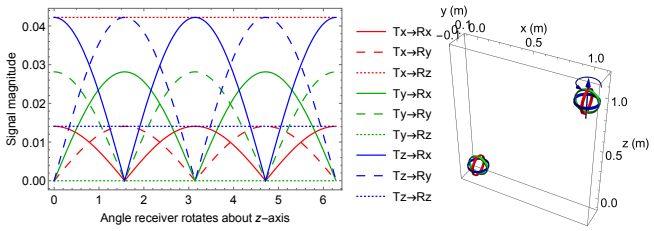

Fig. 2. The induced currents from all three receiving coils as a function of rotation angle as a Rx coil located at $[1, 0, 1]$ rotates about its z-axis.

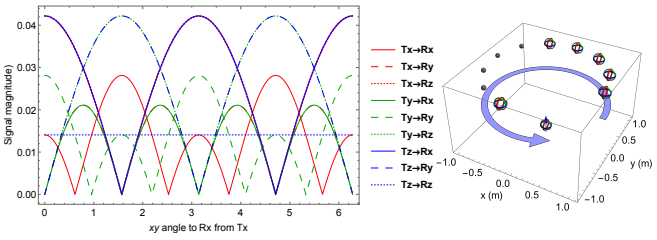

Fig. 3. Signal strength from all three receiving coils as it translates (without rotating) in the $z = 0$ plane around the transmitter coils at a radius of one meter.

generate a magnetic field that is expressed by

$$H(\overrightarrow{r}) = \frac{1}{4\pi|r|^3}[3\widehat{r}(\overrightarrow{m}\cdot\widehat{r}) - \overrightarrow{m}], \tag{1}$$

where $\overrightarrow{r}$ is the distance from the dipole to the observation point and $\overrightarrow{m} = NIA\widehat{u}$ is the magnetic moment of the dipole. For a coil antenna, the magnetic moment is the product of the number of wire turns, the current flowing through the wire, the area of the coil and the unit vector $\widehat{u}$ perpendicular to that area.

The magnetic field generated by each transmitting coil can then be decomposed into its x, y and z components by substituting $\overrightarrow{m}$ into (1). For example, the x magnetic field due to coil i is given by

$$\begin{aligned} H_x^i &= \frac{|\overrightarrow{m}|}{4\pi|r|^3}[3\widehat{r}_x(\overrightarrow{m}^i\cdot\widehat{r}) - \overrightarrow{m}_x^i]\widehat{x} \\ &= \frac{|\overrightarrow{m}|}{4\pi|r|^3}[3\widehat{r}_x(\widehat{m}_x^i\widehat{r}_x + \widehat{m}_y^i\widehat{r}_y) + \widehat{m}_z^i\widehat{r}_z) - \widehat{m}_x^i]\widehat{x} \end{aligned} \tag{2}$$

In total, we have 9 magnetic field components at the receiving antenna. Using those components and (1) we have a total of 9 equations, but the components of $\overrightarrow{r}$ and of $\overrightarrow{m}$ for each coil raise the total number of unknown variables to 12. As a result of the fact that the three coils are orthogonal to each other,

$$\overrightarrow{m}^1\cdot\overrightarrow{m}^2 = \overrightarrow{m}^1\cdot\overrightarrow{m}^3 = \overrightarrow{m}^2\cdot\overrightarrow{m}^3 = 0.$$

However, that approach for extracting the state of the transmitting antenna results in a system with multiple solutions due to the nature of the dot product, so instead we opt for a simpler method that directly extracts the magnitude

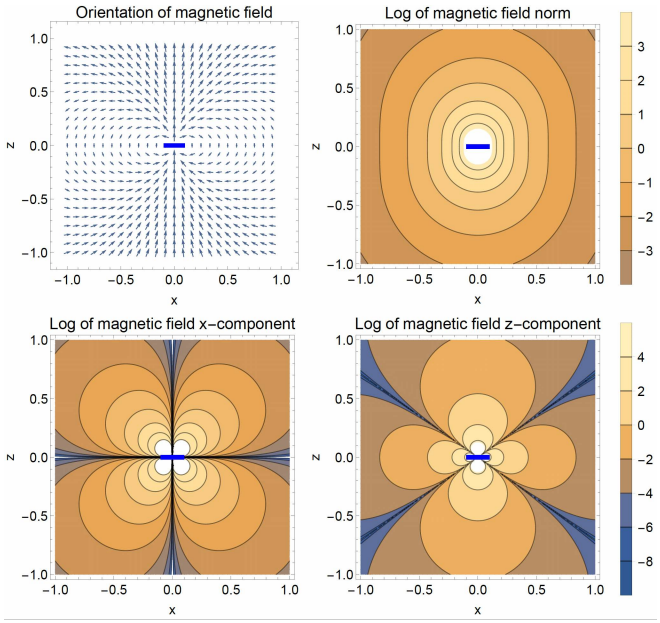

Fig. 4. The magnetic field orientation, magnitude, and magnitude of x and z components for a z-coil. The magnetic field is symmetric about the z axis. The magnetic y component is not shown because the it is zero everywhere in the plane $y = 0$.

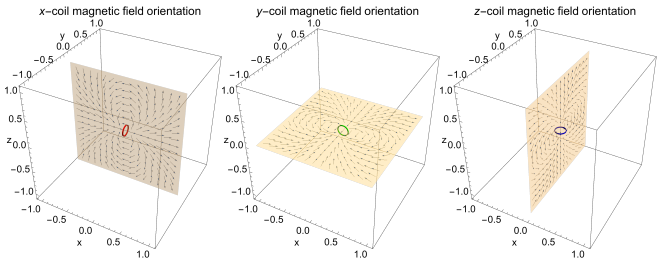

Fig. 5. The magnetic field orientations for x, y, and z coils. The magnetic field has an axis of symmetry in the coil's axial direction, so only a single cut plane is shown for each.

of $\overrightarrow{r}$. We begin by finding the norm of the magnetic field produced by the transmitting coil i. For brevity, we define a new variable q that represents the dot product of $\widehat{r}$ and $\widehat{m}$. The norm of H^i is then given by

$$\begin{aligned} norm(H^i) &= \sqrt{(H_x^i)^2 + (H_y^i)^2 + (H_z^i)^2} \\ &= \frac{|\overrightarrow{m}|}{4\pi|r|^3}\sqrt{(3\widehat{r}_x q^i - \widehat{m}_x^i)^2 + (3\widehat{r}_y q^i - \widehat{m}_y^i)^2 + (3\widehat{r}_z q^i - \widehat{m}_z^i)^2} \\ &= \frac{|\overrightarrow{m}|}{4\pi|r|^3}\sqrt{3(q^i)^2 + 1}. \end{aligned} \tag{3}$$

Since the three transmitting coils are orthogonal, the vector $\overrightarrow{q} = [q^1 q^2 q^3]$ is also a unit vector. By assuming that the magnitude of the magnetic moment of all three coils is the same we get the following system of linear equations:

$$\begin{aligned} 3(\frac{norm(H^1)}{norm(H^2)})^2(q^2)^2 + (\frac{norm(H^1)}{norm(H^2)})^2 &= (3q^1)^2 + 1 \\ 3(\frac{norm(H^1)}{norm(H^3)})^2(q^3)^2 + (\frac{norm(H^1)}{norm(H^3)})^2 &= (3q^1)^2 + 1 \\ (q^1)^2 + (q^2)^2 + (q^3)^2 &= 1 \end{aligned} \tag{4}$$

By solving for $\overrightarrow{q}$ the magnitude of $\overrightarrow{r}$ can be calculated from (3).

To localize the transmitting antenna based only on $|\overrightarrow{r}|$ we employ a particle filter. [14] The particle filter approximates the posterior distribution of the transmitting antenna x_t by a finite number of parameters, in our case the magnetic field components at the receiver. Particle filters represent *bel(x_t)* by a set of random state samples drawn from it. The advantage of sample-based representation is its ability to model nonlinear transformations of random variables. The random state samples are called particles. Each particle is defined by a sample state denoted by the position coordinates x, y, z.

Every time a new set of magnetic filed measurements is taken, the particle filter assigns a probability weight to each particle. Because this is a robotic application we assume we can measure the velocity of the ROVs carrying the antennas. The particles are propagated after their weight is assigned based on the relative velocity of the transmitting ROV with respect to that of the receiving ROV. Repeating this process eventually produces a set of particles representing the locations of the transmitting ROV with highest probability. In every iteration, we also use a Low Variance Sampler to re-sample the particles based on the current probability weights. The algorithm is shown in Algorithm I.

IV. Experiments

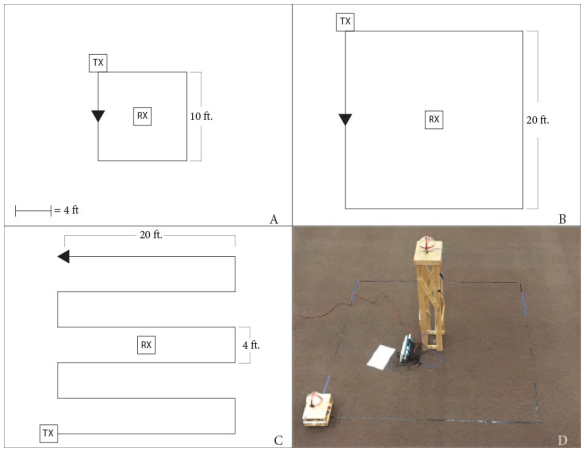

Fig. 6. Experiment setup. (A) Square path with side length of 10 feet. (B) Square path with side length of 20 feet. (C) 20 feet boustrophedon path. (D) The physical setup.

We performed three experiments in air to validate the methods described in this work, as illustrated in Figure 6. The transmitting triaxial antenna moves around the receiving

Algorithm 1 Particle filter using range $|\overrightarrow{r}|$ only

Input: Magnetic field measurements, parameters for calculating magnetic moment of coils

Output: Particles representing locations of transmitting ROV

function PARTICLE FILTER
  Initialize particles and their states
  Initialize probabilistic parameters
  Compute magnetic moment magnitude $|m|$ of coils
  for $t \leftarrow start$ to end **do**
    Take antenna measurements
    Calculate $\overrightarrow{r}$
    for each particle p_i **do**
      Calculate the distance to p_i from receiving ROV
      Compute the probability w_i of the particle with respect to antenna measurements
    end for
    Set particle with highest w_i as current Maximum Likelihood Estimate
    Use Low Variance Sampler to re-sample particles
    Measure current velocity of transmitting ROV $\overrightarrow{v}$
    Propagate particles according to $\overrightarrow{v}$
  end for
end function

triaxial antenna based on three predetermined paths. The first path consists of a 10 by 10 feet square, the second one of a 20 by 20 feet square and the last one of a 20 by 20 feet boustrophedon path. For the first path the receiver was positioned 6 feet above the ground. For the other two paths, the receiver was 3 feet above the ground.

We use an oscilloscope to collect data from the receiving coils as the transmitter moves along the paths. We specify a distance interval the transmitter moves along the paths before taking a measurement. Specifically, the interval is 1 foot for the first path, and 2 feet for the other two paths, for a total of 160 measurement locations. Measurements are logged by turning on each transmitting coil individually and measuring the received voltage signal strength in each receiving coil. We analyze the data after the experiments.

Each coil of our triaxial antennas consists of 29-turn, 24-AWG enameled wire. The self-inductance of each coil is about $370\mu H$. To match the antennas, a capacitor is added in series to the transmitting antenna in order to amplify the excitation current, and in parallel to the receiving antenna in order to increase the impedance. For our working frequency of $125kHz$, the value of the capacitor is about $4.7nF$.

The transmitting circuit for our antenna is shown in Fig. 7. It consists of two operational amplifiers in parallel, one in inverting configuration and the other in non-inverting configuration. Both operational amplifiers have a current boosting stage connected to their outputs because the transmitting antenna can draw several amps of current while in operation. The antenna-capacitor network is connected between the outputs of the operational amplifiers, effectively doubling the voltage across the network because the outputs are out of phase by 180 degrees. The input is provided by a Texas Instrument MSP432 board, and is a $125kHz$ PWM signal. Although the signal is a square wave, the antenna acts as a second order filter that makes the voltage across it nearly sinusoidal. Not shown in the schematic are three relays used to control which of the three transmitting coils is active at any given time, also controlled by the MSP432 board. For power consumption and safety reasons, the input is only active for a short amount of time (just enough to collect an oscilloscope reading) and the relays are only switched when the input is off. Two 4-cell LiPo batteries are used to power the amplifier.

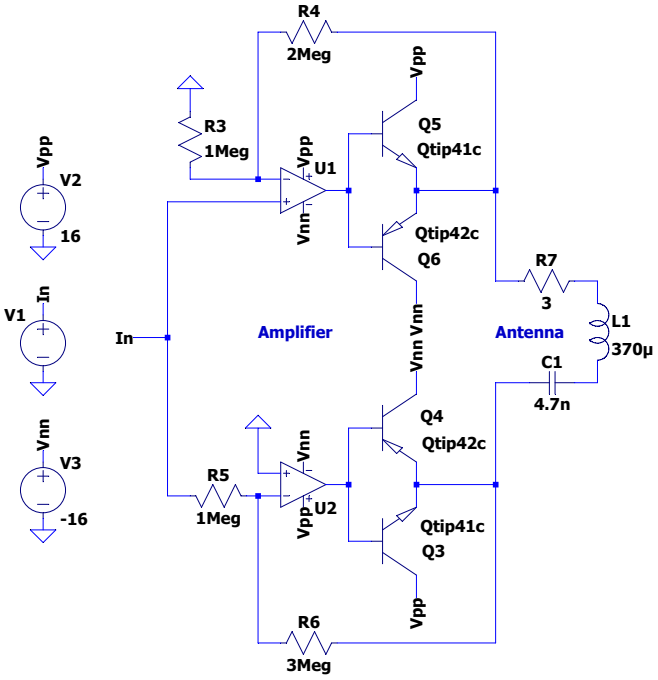

Fig. 7. The driving circuit for the transmitting antenna.

V. RESULTS

Once the voltage measurements are obtained, we convert them into the magnetic field data needed to use (5) to obtain $|\overrightarrow{r}|$. Using Faraday's law we can write the following equation

$$|H| = |V|/\mu_0 NA \tag{5}$$

since we are only concerned with the maximum value of the voltage induced in the receiving coils. In all of our derivations and in the particle filter algorithm we assume and excitation current of $1A$. Because of (3) we can scale the magnetic field data linearly in the case the excitation current of the transmitting coils is different. Using a current probe we measured the average excitation currents of the three transmitting coils to be $[2.082.280.8]A$ so we divided

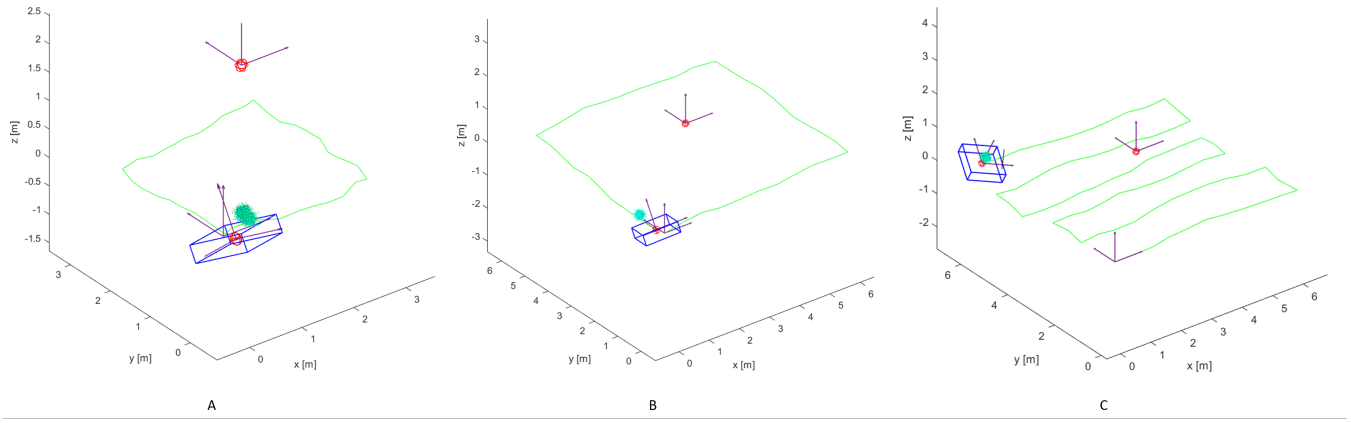

Fig. 8. Localization estimates produced by the particle filter for (A) path 1 (B) path 2 and (C) path 3. The particle cloud (green) can be seen close to the body of the transmitting ROV (blue).

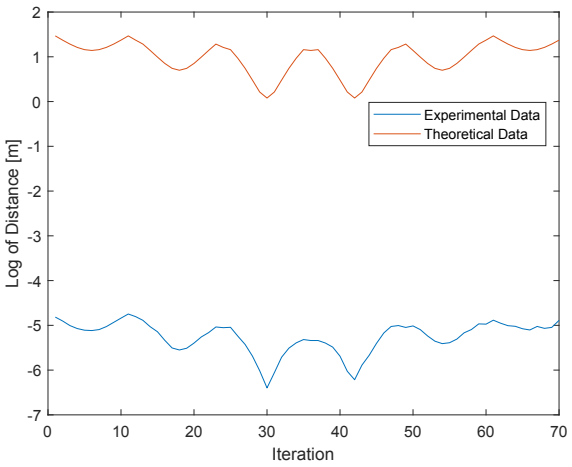

Fig. 9. Log of the calculated $|\overrightarrow{r}|$ for Path 3 based on the experimental data and the theoretical data.

the data accordingly. Unfortunately this shows that our third transmitting coil is potentially faulty, but the algorithm is robust enough to deal with this issue.

Once the data is appropriately converted we input it into a simple program that calculates $|\overrightarrow{r}|$ for every measurement point. Figure 9 shows a comparison of the $|\overrightarrow{r}|$ based on our experimental data, and data created by using the known position of the transmitting antenna and (3). While there is a considerable difference between both plots in terms of magnitude, their overall shapes are similar which indicates we can modify our experimental data to better match the theoretical data by applying a linear hypothesis

$$d_E = \theta_1 d_T + \theta_2 \tag{6}$$

where d_E are the experimental $|\overrightarrow{r}|$ and d_T are the corresponding theoretical values, θ_1 is a scaling factor and θ_2 a variance term. In order to obtain θ_1 and θ_2, all measurement data is taken into account. The mean of d_E/d_T is equal to the scaling factor, and then the variance between $\theta_1 d_E$ and d_T is computed. Based on the data, we have the following values

$$\theta_1 = 2.2(10^{-3})$$
$$\theta_2 = 16.5(10^{-3})$$

Using the hypothesis we can modify the data for the particle filter to work correctly. Since d_E is computed from our measurements and d_T is the true range of the transmitting ROV, we can consider the hypothesis to be the probabilistic model of our measuring technique. This probabilistic model is used by the particle filter to assign the weights that allow it to generate an estimate. The results for the three paths are shown in Figure 8.

It can be seen that the particle cloud corresponding to the location estimation at the end of each path is close to the true state of the transmitting ROV. In order to avoid the particle could from condensing too much, and to capture the uncertainty of an ROV moving in water, a noise term with value of 0.05 was added when propagating the transmitting ROV as well as the particles in the filter. The noise noticeably affects the state of the ROV as it moves, but the overall path is still close to the perfect, noiseless case.

VI. Conclusions

In this work we test the feasibility of using a particle filter to perform robot localization by extracting only range data using triaxial coil antennas. We found that in air we are able to obtain good estimates for the location of the moving transmitting coils for three different paths. The system is robust enough to handle the multiple solutions problem that is caused by using triaxial antennas. Particularly, the orientation of the receiving coils is trivial when calculating $|\overrightarrow{r}|$. In future work we plan to analyze the performance of this system in different mediums, such as underwater and in underground environments, which are the intended application of MI wireless sensor networks. We also intend to further investigate the performance of the particle filter as we take into account sensor data such as depth and orientation of the ROVs in addition to $|\overrightarrow{r}|$.

REFERENCES

[1] "Waterlinked Underwater GPS," https://waterlinked.com/underwater-gps/.

[2] I. F. Akyildiz, P. Wang, and Z. Sun, "Realizing Underwater Communication through Magnetic Induction," *IEEE Communications Magazine*, November 2015.

[3] Y. Li, S. Wang, C. Jin, Y. Zhang, and T. Jiang, "A Survey of Underwater Magnetic Induction Communications: Fundamental Issues, Recent Advances, and Challenges," *IEEE Communications Surveys Tutorials*, February 2019.

[4] F. H. Raab, E. B. Blood, T. O. Steiner, and H. R. Jones, "Magnetic position and orientation tracking system," *IEEE Transactions on Aerospace and Electronic Systems*, vol. AES-15, no. 5, pp. 709–718, Sep. 1979.

[5] F. H. Raab, "Quasi-static magnetic-field technique for determining position and orientation," *IEEE Transactions on Geoscience and Remote Sensing*, vol. GE-19, no. 4, pp. 235–243, Oct 1981.

[6] G. De Angelis, A. De Angelis, V. Pasku, A. Moschitta, and P. Carbone, "A hybrid outdoor/indoor positioning system for iot applications," in *2015 IEEE International Symposium on Systems Engineering (ISSE)*, Sep. 2015, pp. 1–6.

[7] ——, "An experimental system for tightly coupled integration of gps and ac magnetic positioning," *IEEE Transactions on Instrumentation and Measurement*, vol. 65, no. 5, pp. 1232–1241, May 2016.

[8] D. D. Arumugam, J. D. Griffin, D. D. Stancil, and D. S. Ricketts, "Three-dimensional position and orientation measurements using magneto-quasistatic fields and complex image theory [measurements corner]," *IEEE Antennas and Propagation Magazine*, vol. 56, no. 1, pp. 160–173, Feb 2014.

[9] D. D. Arumugam, "Through-the-wall indoor tracking and navigation using deep-sub-wavelength magnetoquasistatics," in *2017 IEEE International Symposium on Antennas and Propagation USNC/URSI National Radio Science Meeting*, July 2017, pp. 1409–1410.

[10] M. Hehn, E. Sippel, C. Carlowitz, and M. Vossiek, "High-accuracy localization and calibration for 5-dof indoor magnetic positioning systems," *IEEE Transactions on Instrumentation and Measurement*, vol. 68, no. 10, pp. 4135–4145, Oct 2019.

[11] G. Dumphart, H. Schulten, B. Bhatia, C. Sulser, and A. Wittneben, "Practical accuracy limits of radiation-aware magneto-inductive 3d localization," in *2019 IEEE International Conference on Communications Workshops (ICC Workshops)*, May 2019, pp. 1–6.

[12] D. Wei, S. Soto, J. Garcia, A. Becker, L. Wang, and M. Pan, "Rov assisted magnetic induction communication field tests in underwater environments," in *WUWNet 2018 - Shenzhen, China*, December 2018.

[13] H. Huang and Y. R. Zheng, "Node localization in 3-d by magnetic-induction communications in wireless sensor networks," in *OCEANS 2017 - Anchorage*, Sep. 2017.

[14] S. Thrun, "Probabilistic robotics," *Commun. ACM*, vol. 45, pp. 52–57, 03 2002.